International Journal of Innovative Computing, Information and Control
Volume **19**, Number **6**, December **2023**

ICIC International ©2023 ISSN 1349-4198
pp. **1933–1952**

MODAL ANALYSIS FOR EVALUATING THE TRANSMISSION OF VERTICAL VIBRATIONS IN A WHEELCHAIR-OCCUPANT MODEL WITH FOAM-BASED SEAT CUSHION

Pongtep Weerapong[1], Mitsuki Katahira[2], Kotaro Hashikura[3]
Md Abdus Samad Kamal[3], Iwanori Murakami[3] and Kou Yamada[3]

[1]Department of Production Technology
Faculty of Industrial Technology
Nakhon Si Thammarat Rajabhat University
M4 Tha-Ngow Subdistrict, Maung District, Nakhon Si Thammarat 80280, Thailand
pongtap_wee@nstru.ac.th

[2]Graduate School of Science and Technology
[3]Division of Mechanical Science and Technology
Gunma University
1-5-1 Tenjincho, Kiryu 376-8515, Japan
{ t221b020; k-hashikura; maskamal; murakami; yamada }@gunma-u.ac.jp

Received February 2023; revised June 2023

Abstract. *An 11-degrees-of-freedom (11-DOF) model is constructed to evaluate the transmission of vertical vibrations in wheelchair-occupant systems. Modal analysis is employed to develop reliable dynamic models that predict the steady-state response accurately. The modal analytical method demonstrates high accuracy by successfully predicting seat transmissibility and comparing favorably with published results. Analysis identifies the occupant's torso as having the highest amplitude ratio of transmissibility responses, facilitating the identification of vibration phenomena. A linear differential equation model with 11 degrees of freedom effectively predicts the behavior of foam-based cushions in vibration and shock absorption. Comparisons with experimental data validate the model's performance. This modeling approach has significant potential for advancing wheelchair design and analyzing vibrating systems. Future research can further enhance the model by incorporating complex geometries and material properties, coupled with experimental validation. Addressing limitations and pursuing suggested directions will improve accuracy, reliability, and applicability, contributing to a deeper understanding of vibration transmissibility and prioritizing occupant comfort and safety in wheelchair systems.*
Keywords: Modal analysis approach, Wheelchair-occupant system, Vibration, Seat cushion, Goodness-of-fit, Transmissibility

1. **Introduction.** Numerous studies have extensively examined the impact of vibrations on wheelchair-occupant systems, revealing the adverse consequences of these vibrations on the wheelchair and, more particularly, the rider. Such vibrations can result in discomfort and compromise the stability of the vehicle, thereby posing potential health hazards to the users [1, 2, 3]. Among different types of vibrations, vertical vibrations have emerged as particularly problematic within wheelchair operating environments, leading to the most severe outcomes [4, 5, 6]. Moreover, wheelchair users who rely on wheelchairs and already have pre-existing physical conditions or long-term illnesses face amplified risks associated with vibrations. The medical community has well-established the detrimental effects of sustained vibrations on vital organs like the heart, lungs, rib cage, and brain. For example,

DOI: 10.24507/ijicic.19.06.1933

vibrations can trigger movement within the skull, potentially resulting in internal brain hemorrhage. Furthermore, vibrations can cause damage to soft tissues in the intestines and rectum, as well as strain tendons and joints. Extended exposure to vibrations has been associated with various neurological and physiological effects, including conditions such as arthritic joints, lower back pain, and other musculoskeletal syndromes [1, 5, 7].

The primary focus of this study was to examine the impact of vertical vibrations on the wheelchair and occupant unit, specifically how they affect the occupant's body. In order to assess the transmission of vibrating forces, the study aimed to analyze the relationship between seat parameters and the dynamic response of the seat in terms of acceleration or displacement ratios [8, 9, 10, 11, 12, 13, 14]. To validate the model used in this study, the results were compared to the findings of Garcia-Mendez et al. [8], who investigated the human body response in various vehicle seats using a multi-body biodynamic model. Previous research papers have also explored the issue of vibration transmission and its effects on the human body, employing mathematical simulations and analyzing lumped parameters of a seated human model [15]. These models typically segment the human body into different parts, such as the head, back, torso, thorax, diaphragm, abdomen, and pelvis, treating them as interconnected masses, springs, and dampers [8, 10, 11, 12, 13, 14]. These models consider the forces involved in the movement of the torso relative to the back, as well as other forces acting directly on the seated human form. For instance, Weerapong et al. [13, 14] applied an 11-DOF model to studying the biodynamic responses of a seated wheelchair occupant exposed to vertical vibrations during driving conditions. Liang and Chiang [16], inspired by Patil's model, divided the occupant's body into three parts and compared the biodynamics of the seated posture without backrest support by analyzing several lumped parameters to determine seat-to-head transmissibility. Similarly, Nangolo et al. [17] developed a model with a 9-DOF, 4-axle freight wagon system, employing combined modal analysis and numerical integration of convolution integrals using piecewise constants as interpolating functions. By contrast, Schwochow and Jelcic [18] applied operational modal analysis methods to studying vibration transmissibility during ground vibration tests of an aircraft, focusing on the analysis of output acceleration response.

The primary motivation of this work was to explore the application of modal analysis techniques in constructing and representing dynamic mechanical models for transmissibility testing and comparing displacement ratios to calculate human dynamic responses. Modal analysis offers a powerful approach to understanding the complex dynamics of mechanical systems by decomposing them into individual vibration modes [19, 20]. In this study, we focused on developing an 11-DOF model that represents the linear lumped parameters of a seated human form. This model was specifically designed to investigate the effects of mechanical stiffness and damping in wheelchair seat suspensions on the occupant. By employing combinations of individual vibration modes, we aimed to accurately capture the dynamic behavior of the system. It is important to acknowledge that our simulation was confined to evaluating the dynamic response of a human exposed to vertical vibrations. It should be noted that our model is not intended to be a general-purpose human biodynamic model encompassing all possible scenarios and vibrations. Instead, we aimed to create a simplified representation that allows us to determine displacement ratio values relevant to a human dynamic response model [2, 3, 4]. By utilizing this approach, we sought to contribute to the understanding of how mechanical factors, specifically stiffness and damping in wheelchair seat suspensions, impact the dynamic responses experienced by the occupant. This knowledge has practical implications for the design and development of more supportive and comfortable seating systems for wheelchair users. Ultimately, our work aims to improve the overall well-being and comfort of individuals

exposed to vibrations by providing insights into the influence of mechanical parameters on their dynamic responses.

This paper is organized in sections. Section 2 analyzes the wheelchair and occupant regarding properties of human tissue, spring and damper, and defines the force vectors upon the masses in the free body diagram. Section 3 has the model's equations of motions (EOMs) rearranged, using Fourier transformation and Euler's formula, into matrices containing equations and frequency response functions. Section 4 concerns the evaluation and validation of the wheelchair-occupant model; and application of transmissibility and the displacement responses to assess the prediction accuracy of the model. Section 5 delivers concluding remarks.

2. **Analysis of Lumped Mechanical System.** Construction of the occupant-wheelchair system is outlined in Figure 1 which serves as the foundation for the technical analysis and modeling in this study. The model consists of 11 masses representing various components of the system, including the head, back, torso, thorax, diaphragm, abdomen, pelvis, seat cushion, front tires, and rear tires. To accurately capture the complex dynamics and interactions within the system, 13 damping coefficients (c) and 13 spring constants (k) are introduced. These damping coefficients and spring constants connect the 11 masses, enabling the representation of the interconnectedness and interdependencies between the different components. Moreover, a novel approach is employed to simulate the system's response to external input. Instead of utilizing sinusoidal excitation force input, the input displacement $y_0 = y_0 \sin(\omega t)$ is used. This represents the motion of the ground surface, such as road roughness or uneven terrain. The input displacement affects both the front tires and the rear tires, as well as the connecting springs and dampers. The equation of motion for the front tires describes their motion based on the forces exerted by the suspension system, the ground input, and the connecting springs and dampers. The last two terms on the right-hand side of the equation represent the excitation due to road roughness. Here, y_0 represents the road input amplitude, and ω represents the

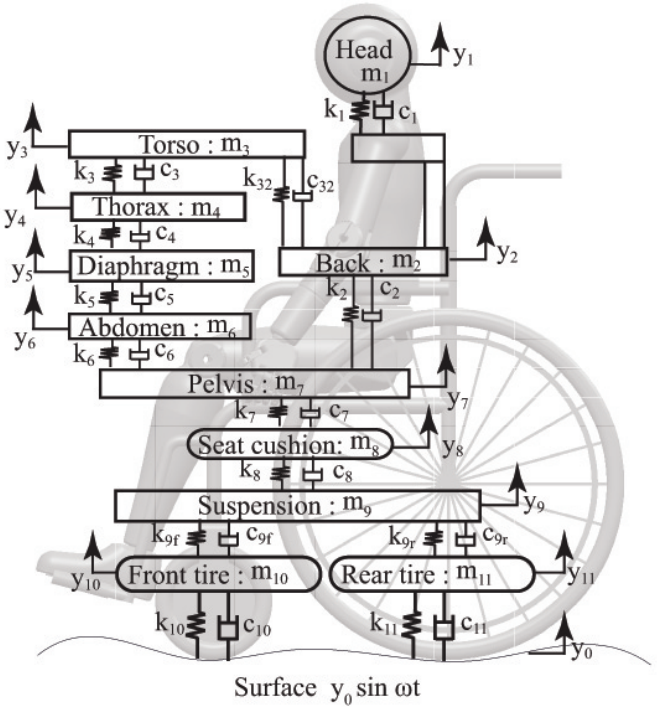

FIGURE 1. Eleven lumped-mass models of wheelchair-occupant system

frequency of the road input. Similarly, the equation of motion for the rear tires accounts for the forces exerted by the suspension system, the ground input, and the connecting springs and dampers. The last two terms on the right-hand side of the equation represent the excitation resulting from road roughness. By incorporating these additional damping coefficients, spring constants, and modifying the input displacement, the model addresses the technical challenge of accurately representing the intricate dynamics of the wheelchair-occupant system, particularly in response to real-world road conditions and variations in the terrain.

An in-depth investigation of a lumped mechanical system. A meticulous analysis of a lumped mechanical system is presented in this paper, focusing on the detailed construction of the wheelchair-occupant system shown in Figure 1. The system is modeled as a typical manual appliance, where the occupant's lower segment(s) are supported by the seat cushion while the upper segments remain unsupported by a backrest. Input vibrations are limited to sinusoidal functions transmitted through the seat cushion from the springs and dampers on the wheelchair tires. The amplitude of the input wave is set at 0.005 [mm]. Real-world vibrations transmitted through the wheelchair foot support are disregarded due to their negligible magnitude. Figure 1 depicts a cross-section of the wheelchair and occupant, featuring eleven mass blocks labeled as m_i ($i = 1, \ldots, 11$). These blocks are connected in pairs by springs and dampers, with their stiffness and damping coefficients represented by k_i and c_i, respectively. The values of these coefficients are derived from previously published experimental results, which can be found in Tables 1 and 2. The occupant is modeled as a 7-DOF frame, based on the work of Liang and Chiang [16], which represents an idealized sitting human anatomy. The parts of the occupant's body are considered as isolated masses connected at the joints where relative movements are allowed. The seven blocks representing the head (m_1), back (m_2), torso (m_3), thorax (m_4), diaphragm (m_5), abdomen (m_6), and pelvis (m_7) are interconnected by springs and dampers, capturing the resilient characteristics of the connective tissues between these components. The parameter values for these human tissues are obtained from various studies on anatomical subsystems and are documented in Table 1. The 4-DOF wheelchair is represented by four blocks: 1) the seat, padded with a cushion of negligible mass; 2) suspension; 3) front tires; and 4) rear tires – these, as denoted by m_8, m_9, m_{10}, and m_{11}, are listed in Table 2. The analysis presented in this paper provides a comprehensive understanding of the complex dynamics exhibited by the wheelchair-occupant system.

Table 1. Parameter values of occupant model [16]

Mass [M] (kg)	Damping constant [C] (N/m/sec)	Spring constant [K] (N/m)
$m_7 = 27.7$	$c_7 = 378$	$k_7 = 25500$
$m_6 = 6.02$	$c_6 = 298$	$k_6 = 894.1$
$m_5 = 0.46$	$c_5 = 298$	$k_5 = 894.1$
$m_4 = 1.38$	$c_4 = 298$	$k_4 = 894.1$
$m_3 = 33.33$	$c_3 = 298$	$k_3 = 894.1$
	$c_{32} = 3651$	$k_{32} = 53640$
$m_2 = 6.94$	$c_2 = 3651$	$k_2 = 53640$
$m_1 = 5.5$	$c_1 = 3651$	$k_1 = 53640$

TABLE 2. Parameter values of manual wheelchair [8, 21]

Mass $[M]$ (kg)	Damping constant $[C]$ (N/m/sec)	Spring constant $[K]$ (N/m)
$m_{11} = 1.6$	$c_{11} = 500$	$k_{11} = 6000$
$m_{10} = 1.0$	$c_{10} = 500$	$k_{10} = 60000$
$m_9 = 15$	$c_{9f} = 700$	$k_{9f} = 13400$
	$c_{9r} = 700$	$k_{9r} = 74600$
$m_8 = 1.5$	$c_{8a} = 1689$	$k_{8a} = 183200$
input magnitude vibration, $y_0 = 5.0$ [mm].		

f and r denote the parameter values for suspension f, for front; r, for rear.
a denotes the parameter value for Comfort Mate Foam, a commercial cushion brand.

3. **Modeling Approach and Experimental Measurements.** This paper introduces a novel technique for evaluating the transmission of vertical vibrations in a wheelchair-occupant system, which distinguishes itself from existing literature in several key aspects. Firstly, it utilizes an 11-DOF model, offering a more comprehensive representation of the system dynamics compared to previous studies. By considering additional DOFs, such as the diaphragm and abdomen, this model provides a more accurate depiction of the occupant's response to vibrations. Furthermore, this work incorporates a foam-based cushion model, which is an innovative addition not commonly found in the literature. The inclusion of the cushion model enables a more realistic simulation of the interaction between the occupant and the seat, considering the impact of cushion properties on vibration transmission. This aspect of the study contributes to a more precise understanding of the factors influencing transmissibility. The use of modal analysis is another distinguishing feature of this research. By applying modal analysis techniques, reliable and validated dynamic models are developed, providing a solid foundation for further analysis [17, 19, 20]. This approach ensures that the predicted steady-state response aligns closely with the actual measured seat transmissibility, enhancing the accuracy and reliability of the findings. Comparisons with published results further validate the effectiveness of the modal analytical method employed in this study. Moreover, the focus on the amplitude ratio of transmissibility responses in the occupant's torso is an incremental point highlighted in this work. By identifying and evaluating vibration phenomena in the torso, this analysis sheds light on the specific areas of the body that are most susceptible to vibrations. This information is valuable for understanding the potential impact on the occupant's comfort and well-being, as well as informing the design of interventions or improvements to mitigate excessive vibrations.

3.1. **Derivation of EOMs in matrix form.** In this section, we describe the mathematical model used to analyze the dynamics of the system depicted in Figure 1. The equations of motion (EOMs) are derived in Fourier transformation and presented in matrix form, incorporating mass, inertia, and forces generated by springs and dashpots. The EOMs can be expressed as follows:

$$[M]\{\ddot{y}(t)\} + [C]\{\dot{y}(t)\} + [K]\{y(t)\} = [[C_0]\{\dot{y}_0(t)\} + [K_0]\{y_0(t)\}] \sin \omega t, \tag{1}$$

$$[[C_0]\{\dot{y}_0(t)\} + [K_0]\{y_0(t)\}] \sin \omega t = \{F(t)\}. \tag{2}$$

Here, the matrices $[M]$, $[K]$, and $[C]$ are 11×11 matrices representing mass, stiffness, and damping, respectively. The displacement, velocity, and acceleration vectors of the response are denoted by $y(t)$, $\dot{y}(t)$, and $\ddot{y}(t)$, respectively. The excitation frequency is denoted by ω. To gain a deeper understanding of the EOMs, let us examine the individual terms and their

origins. The elements of matrices $[M]$, $[K]$, and $[C]$ are derived from the EOMs presented in Equations (3) to (13). The mass matrix contains zero elements except for the diagonal terms, indicating that only the diagonal terms contribute to the mass-related forces. The excitation stiffness and damping matrices, represented by $[K_0]$ and $[C_0]$, respectively, are 11×1 matrices with zero elements except for the 10th and 11th rows. These specific rows correspond to the sinusoidal forces described in Equations (12) and (13), representing the forces exerted on the system due to external excitation. In summary, the matrix-form EOMs provide a concise representation of the system's dynamics, encompassing the effects of mass, stiffness, damping, and external forces. These equations serve as the basis for analyzing the behavior of the wheelchair-occupant system and can be further solved to determine the system's response under various conditions.

3.2. **The system of equations of motion for the 11-DOF wheelchair-occupant model.** These EOMs are summarized as

1. The head

$$m_1\ddot{y}_1 = c_1(\dot{y}_2 - \dot{y}_1) + k_1(y_2 - y_1), \tag{3}$$

where i) m_1, c_1, k_1, $\ddot{y}_1$, $\dot{y}_1$ and y_1 are the mass, damping, spring, acceleration, velocity and displacement of the head, ii) $\dot{y}_2$ and y_2 are, respectively, the velocity and displacement of the back.

2. The back

$$\begin{aligned} m_2\ddot{y}_2 = {} & c_1(\dot{y}_1 - \dot{y}_2) + c_{32}(\dot{y}_3 - \dot{y}_2) + c_2(\dot{y}_3 - \dot{y}_2) + k_1(y_1 - y_2) + k_2(y_3 - y_2) \\ & + k_{32}(y_3 - y_2), \end{aligned} \tag{4}$$

where i) m_2, c_2, k_2, $\ddot{y}_2$, $\dot{y}_2$ and y_2 are the mass, damping, spring, acceleration, velocity and displacement of the back, ii) c_{32}, k_{32} are, respectively, the damping and spring constants of tissue between the torso and back, iii) $\dot{y}_3$, y_3 refer to the velocity and displacement of the torso, respectively.

3. The torso

$$m_3\ddot{y}_3 = c_{32}(\dot{y}_2 - \dot{y}_3) + c_3(\dot{y}_4 - \dot{y}_3) + k_{32}(y_2 - y_3) + k_3(y_4 - y_3), \tag{5}$$

where i) m_3, c_3, k_3, and $\ddot{y}_3$ are the mass, damping, spring, and acceleration of the torso, ii) $\dot{y}_4$, y_4 refer to the velocity and displacement of the thorax, respectively.

4. The thorax

$$m_4\ddot{y}_4 = c_3(\dot{y}_3 - \dot{y}_4) + c_4(\dot{y}_5 - \dot{y}_4) + k_3(y_3 - y_4) + k_4(y_5 - y_4), \tag{6}$$

where i) m_4, c_4, k_4, and $\ddot{y}_4$ are the mass, damping, spring, and acceleration of the thorax, ii) $\dot{y}_5$, y_5 refer to the velocity and displacement of the diaphragm, respectively.

5. The diaphragm

$$m_5\ddot{y}_5 = c_4(\dot{y}_4 - \dot{y}_5) + c_5(\dot{y}_6 - \dot{y}_5) + k_4(y_4 - y_5) + k_5(y_6 - y_5), \tag{7}$$

where i) m_5, c_5, k_5, and $\ddot{y}_5$ are the mass, damping, spring, and acceleration of the diaphragm, ii) $\dot{y}_6$, y_6 refer to the velocity and displacement of the abdomen, respectively.

6. The abdomen

$$m_6\ddot{y}_6 = c_5(\dot{y}_5 - \dot{y}_6) + c_6(\dot{y}_7 - \dot{y}_6) + k_5(y_5 - y_6) + k_6(y_7 - y_6), \tag{8}$$

where i) m_6, c_6, k_6, and $\ddot{y}_6$ are the mass, damping, spring, and acceleration of the abdomen, ii) $\dot{y}_7$, y_7 refer to the velocity and displacement of the pelvis, respectively.

7. The pelvis

$$\begin{aligned} m_7\ddot{y}_7 = {} & c_6(\dot{y}_6 - \dot{y}_7) + c_7(\dot{y}_2 - \dot{y}_7) + c_2(\dot{y}_2 - \dot{y}_7) + k_6(y_6 - y_7) + k_7(y_2 - y_7) \\ & + k_2(y_2 - y_7), \end{aligned} \tag{9}$$

where i) m_7, c_7, k_7, and $\ddot{y}_7$ are the mass, damping, spring, and acceleration of the abdomen, ii) $\dot{y}_8$, y_8 refer to the velocity and displacement of the seat cushion, respectively.

8. The seat cushion

$$m_8\ddot{y}_8 = c_7(\dot{y}_7 - \dot{y}_8) + c_8(\dot{y}_9 - \dot{y}_8) + k_7(y_7 - y_8) + k_8(y_9 - y_8), \tag{10}$$

where i) m_8, c_8, k_8, and $\ddot{y}_8$ are the mass, damping, spring, and acceleration of the seat cushion, ii) $\dot{y}_9$, y_9 refer to the velocity and displacement of the suspension, respectively.

9. The suspension

$$\begin{aligned} m_9\ddot{y}_9 = {} & c_8(\dot{y}_8 - \dot{y}_9) + c_{9f}(\dot{y}_{10} - \dot{y}_9) + c_{9r}(\dot{y}_{11} - \dot{y}_9) + k_{9r}(y_{11} - y_9) + k_{9f}(y_{10} - y_9) \\ & + k_8(y_8 - y_9), \end{aligned} \tag{11}$$

where i) m_9, c_{9r}, and k_{9r} are the mass, damping, and spring of the rear suspension, ii) c_{9f} and k_{9f} are damping and spring of the front suspension, iii) $\ddot{y}_9$ is acceleration of the suspension, and iv) $\dot{y}_{10}$ and y_{10} refer to the velocity and displacement of the front tires, respectively, v) $\dot{y}_{11}$ and y_{11} refer to the velocity and displacement of the rear tires, respectively

10. The front tires

$$\begin{aligned} m_{10}\ddot{y}_{10} = {} & c_{9f}(\dot{y}_9 - \dot{y}_{10}) + c_{10}(\dot{y}_0 - \dot{y}_{10}) + k_{9f}(y_9 - y_{10}) + k_{10}(y_0 - y_{10}) \\ & + c_{10}y_0\omega\cos\omega t + k_{10}y_0\sin\omega t \end{aligned} \tag{12}$$

where i) m_{10} is the mass of the front tires, ii) $\ddot{y}_{10}$ refers to the acceleration of the tires, iii) c_{10} and k_{10} are, respectively, the damping and spring constant of front tires. iv) $\dot{y}_0$ and y_0 refer, respectively, to the input velocity and displacement of the tires contact points to the floor. The floor surface will cause the tires to compress, v) y_0, ω are, respectively, the amplitude of input displacement excitation and circular frequency of this displacement applied at the tire contact points to the floor. And

11. The rear tires

$$\begin{aligned} m_{11}\ddot{y}_{11} = {} & c_{9r}(\dot{y}_9 - \dot{y}_{11}) + c_{11}(\dot{y}_0 - \dot{y}_{11}) + k_{9r}(y_9 - y_{11}) + k_{11}(y_0 - y_{11}) \\ & + c_{11}y_0\omega\cos\omega t + k_{11}y_0\sin\omega t, \end{aligned} \tag{13}$$

where i) m_{11} is the mass of the rear tires, ii) $\ddot{y}_{11}$ refers to the acceleration of the rear tires, iii) c_{11} and k_{11} are, respectively, the damping and spring constant of rear tires. This equation describes the motion of the rear tires based on the forces exerted by the suspension system, the ground input, and the connecting springs and dampers. Similar to the front tires, the last two terms on the right-hand side represent the excitation due to road roughness. In terms of the variables used, y_0 and $\dot{y}_0$ represent input displacement and velocity. y_1, $\dot{y}_1$ and $\ddot{y}_1$ represent displacement, velocity and acceleration of the head. y_2, $\dot{y}_2$ and $\ddot{y}_2$ represent displacement, velocity and acceleration of the back. y_3, $\dot{y}_3$ and $\ddot{y}_3$ represent displacement, velocity and acceleration of the torso. y_4, $\dot{y}_4$ and $\ddot{y}_4$ represent displacement, velocity and acceleration of the thorax. y_5, $\dot{y}_5$ and $\ddot{y}_5$ represent displacement, velocity and acceleration of the diaphragm. y_6, $\dot{y}_6$ and $\ddot{y}_6$ represent displacement, velocity and acceleration of the abdomen. y_7, $\dot{y}_7$ and $\ddot{y}_7$ represent displacement, velocity and acceleration of the pelvis. y_8, $\dot{y}_8$ and $\ddot{y}_8$ represent displacement, velocity and acceleration of the seat cushion. y_9, $\dot{y}_9$ and $\ddot{y}_9$ represent displacement, velocity and acceleration of the suspension. y_{10}, $\dot{y}_{10}$ and $\ddot{y}_{10}$ represent displacement, velocity and acceleration of the front tires. And y_{11}, $\dot{y}_{11}$ and $\ddot{y}_{11}$ represent displacement, velocity and acceleration of the rear tires.

These equations of motion describe the dynamic behavior of the 11-DOF wheelchair-occupant model. They relate the accelerations ($\ddot{y}_i$) of each degree of freedom (DOF) to the corresponding forces and displacements. By solving these equations, one can analyze

and simulate the motion and response of the wheelchair-occupant system under various conditions and inputs.

3.3. **The concept of eigenvalue and eigenvector.** In this section, we focus on solving undamped eigenvalues, which plays a crucial role in determining the resonant frequencies (eigenvalues) and mode shapes (eigenvectors) of a system. To accomplish this, we start by deriving the undamped homogeneous (unforced) equations of motion for the model, which can be represented as

$$[M]\{\ddot{y}(t)\} + [K]\{y(t)\} = 0. \tag{14}$$

Due to the conservative nature of the system, we expect the existence of normal modes of vibration. Normal modes imply that at specific frequencies, all points in the system vibrate at the same frequency and phase. Mathematically, normal modes can be expressed as [22]

$$\{y(t)\} = \{u(t)\}\sin(\omega t) = \{u(t)\}Im\left(e^{i\omega t}\right). \tag{15}$$

Here, $\{y(t)\}$ represents the vector of displacements for all degrees of freedom (DOF) at the given frequency, $\{u(t)\}$ represents the i-th eigenvector, which corresponds to the mode shape for the resonant frequency, and ω represents the eigenvalue or resonant frequency. To obtain the steady-state response, we apply Fourier transformation using Euler's formula $e^{i\omega t} = \cos\omega t + i\sin\omega t$, and then substitute the transforms into the steady-state response equation (1). By substituting the exponential function vectors of response $\{y(t)\} = \{u(t)\}e^{i\omega t}$ into Equation (14) and canceling out the exponential terms, we obtain

$$[K]\{u(t)\} = -\omega^2[M]\{u(t)\}. \tag{16}$$

Rewrite the nonstandard form eigenvalue problem as a homogeneous equation:

$$\left([K] - \omega^2[M]\right)\{u(t)\} = 0. \tag{17}$$

During the analysis of the system's eigenvalues, it is noted that a trivial solution, $\{u(t)\} = 0$, exists but does not hold any significance in this context. The nontrivial solutions arise when the determinant of the coefficient matrix is equal to zero [23], resulting in a polynomial equation in ω known as the characteristic equation. The roots of this polynomial correspond to the eigenvalues or resonant frequencies of the system. For each pair of eigenvalues, there is a corresponding eigenvector $[u(t)]$ that characterizes the mode shape of vibration at that specific frequency. To determine the eigenvector, one of the degrees of freedom, denoted as ω, is selected as a reference. By substituting this value into all equations of motion except one, the eigenvector can be obtained. The mode shape matrix $[u] \in R^{11\times 11}$ is then formed by combining the eigenvectors associated with each pair of eigenvalues and written as

$$[u] = 10^{-4} * \begin{bmatrix} 977 & 580 & -123 & -116 & -751 & 362 & 178 & 1 & 0 & 0 & 0 \\ 968 & 567 & -111 & -98 & -513 & 15 & 119 & -338 & -5 & -1 & 3 \\ 104 & 623 & 39 & -101 & 566 & 20 & -392 & 204 & 0 & 0 & 0 \\ 149 & -105 & 773 & 102 & -141 & -2955 & -50 & 0 & 0 & 0 & 0 \\ 173 & -237 & 441 & 679 & -174 & 137 & -53 & 0 & 0 & 0 & 0 \\ 189 & -343 & -992 & -188 & 70 & -501 & -10 & 0 & 0 & 0 & 0 \\ 880 & 483 & -237 & 853 & -115 & -11 & -659 & 257 & 18 & 3 & -49 \\ 572 & 330 & -237 & 149 & 134 & 5 & 99 & 24 & -988 & -243 & 782 \\ 529 & 308 & -236 & 156 & 165 & 7 & 199 & -14 & -686 & -131 & -734 \\ 97 & 56 & -44 & 292 & 315 & 1 & 40 & -4 & -489 & 998 & 127 \\ 490 & 287 & -222 & 149 & 163 & 7 & 212 & -30 & 755 & 263 & 341 \end{bmatrix}. \tag{18}$$

3.4. **Modal expansion theorem.** The modal expansion theorem is a fundamental concept in modal analysis of vibrating systems. It states that any motion set $\{y(t)\}$ can be represented as a combination of individual modes, each characterized by its mode shape u and time-dependent behavior [17, 18]. Mathematically, this theorem can be expressed using Equation (19):

$$\{y(t)\} = \sum_{i=1}^{n} [u_i]\{q_i(t)\}, \tag{19}$$

where $y(t)$ represents the motion set, n is the number of modes, u_i is a coefficient representing the magnitude of the i-th mode shape, and $q_i(t)$ is the time-dependent behavior of the i-th mode.

$$\{y(t)\} = \{u\}^{(1)} q_1(t) + \cdots + \{u\}^{(n)} q_n(t) = \left[\{u\}^{(1)} \dots \{u\}^{(n)}\right] \{q_1(t) \dots q_n(t)\}^T. \tag{20}$$

Equation (20) represents the total response of the system as a superposition of the response of the natural modes of the system. For an n-DOF system there will be n-natural modes, where $\{y(t)\}$ represent generalized coordinates, $[u]$ represent modal coordinate or natural coordinates, and $\{q(t)\}$ represents displacement vector in principal coordinates.

$$\begin{cases} \{y(t)\} = [u]\{q(t)\} \\ \{\dot{y}(t)\} = [u]\{\dot{q}(t)\} \\ \{\ddot{y}(t)\} = [u]\{\ddot{q}(t)\} \end{cases}. \tag{21}$$

Successive differentiations of (20) yield $\{y(t)\}, \{\dot{y}(t)\}, \{\ddot{y}(t)\}$ of Equation (21). Plugging them into Equation (1), and multiplying by $[u]^T$ gives us Equation (22)

$$[u]^T[M][u]\{\ddot{q}(t)\} + [u]^T[C][u]\{\dot{q}(t)\} + [u]^T[K][u]\{q(t)\} = [u]^T\{F(t)\} = \{Q(t)\}, \tag{22}$$

$$[u]^{(s)T}[M][u]^{(r)} = 0 \text{ for } r \neq s. \tag{23}$$

In Equation (23) it is important to note that in order for the equation to hold, matrix $[u]$ must satisfy the condition where the transpose of $[u]$ includes one row from $[u]^{(s)T}$ and one column from u, with the exception of the case when r is equal to s. When this condition is met, the following relationships hold:

$$[u]^T[M][u] = [M_d] = \begin{bmatrix} m_{1d} & 0 & \dots & 0 \\ 0 & m_{2d} & \dots & 0 \\ \vdots & \vdots & \ddots & \vdots \\ 0 & 0 & \dots & m_{11d} \end{bmatrix}, \tag{24}$$

$$[u]^T[K][u] = [K_d] = \begin{bmatrix} k_{1d} & 0 & \dots & 0 \\ 0 & k_{2d} & \dots & 0 \\ \vdots & \vdots & \ddots & \vdots \\ 0 & 0 & \dots & k_{11d} \end{bmatrix}, \tag{25}$$

$$[u]^T[C][u] = [C_d] = \begin{bmatrix} c_{1d} & 0 & \dots & 0 \\ 0 & c_{2d} & \dots & 0 \\ \vdots & \vdots & \ddots & \vdots \\ 0 & 0 & \dots & c_{11d} \end{bmatrix}. \tag{26}$$

It is worth mentioning that $[M_d]$ and $[K_d]$ are diagonal matrices, while $[C_d]$ may not be diagonal in all cases, depending on specific conditions. For Rayleigh damping, the damping matrix $[C]$ can be obtained as a linear combination of the stiffness matrix $[K]$ and mass

matrix $[M]$, i.e., $[C] = \alpha[M] + \beta[K]$. In the context of flexible structures, approximations for viscous damping are also available, as shown in Equations (27) and (28).

$$[u]^T[C][u] = \alpha[M_d] + \beta[K_d], \tag{27}$$

$$[c_{d(kl)}] = \alpha[m_{d(kl)}] + \beta[k_{d(kl)}], \quad k, l = 1, \ldots, 11. \tag{28}$$

$$[M_d]\{\ddot{q}(t)\} + [C_d]\{\dot{q}(t)\} + [K_d]\{q(t)\} = [u]^T\{F(t)\} = \{Q(t)\}. \tag{29}$$

We use the equation of motion in our generalized coordinates, as shown in Equation (29), where $[M_d]$ represents diagonal principal mass matrix (11×11), [Kg]. $[K_d]$ represents diagonal principal stiffness matrix (11×11), [N/m]. $[C_d]$ represents diagonal principal damping matrix (11×11), [Ns/m]. $\{\ddot{q}(t)\}$ represents acceleration vector in principal coordinates (11×1), [m^2/s]. $\{\dot{q}(t)\}$ represents velocity vector in principal coordinates (11×1), [m/s]. $\{q(t)\}$ represents displacement vector in principal coordinates (11×1), [m]. $\{Q(t)\}$ represents force transpose of vector in principal coordinates (11×1), [N/m^2].

3.5. **Matrix formulation of the complex fourier transform.** The complex Fourier transform can be expressed using Euler's formula, where $e^{i\omega t} = \cos\omega t + i\sin\omega t$. These transformations are then utilized to substitute into (29) representing the steady-state response. To incorporate the derivatives of the excitation and response equations, we have $\{q_0(t)\} = \{q_0(i\omega)\}e^{i\omega t}$ and $\{q(t)\} = \{q(i\omega)\}e^{i\omega t}$, respectively. By substituting the exponential function vectors $q_0(t)$, $\dot{q}_0(t)$, $q(t)$, $\dot{q}(t)$, $\ddot{q}(t)$ into (1), we obtain the matrix equation that describes the multiple degree of freedom (MDOF) system as follows:

$$\left[-\omega^2[M_d] + i\omega[C_d] + [K_d]\right]\{q\}e^{i\omega t} = \{Q(i\omega)\}e^{i\omega t}. \tag{30}$$

3.6. **Solving for displacement in the complex domain.** The equations of motion (EOMs) of the 11-DOF system are substituted into the complex terms within the transfer function, as expressed in hertz, in Equation (30). By further manipulating this equation, we can eliminate the time-dependent component, resulting in

$$\{q_k(i\omega)\} = \frac{\{Q_l(i\omega)\}}{[-\omega^2[M_d] + i\omega[C_d] + [K_d]]}, \tag{31}$$

where $\{q(i\omega)\}$ and $\{Q(i\omega)\}$ are the corresponding complex Fourier transform vectors of $q_k(i\omega)$ and $Q_l(i\omega)$, respectively. The mass, damping, and stiffness matrices for the body and wheelchair segments are denoted as $[M_d] = [m_{d(kl)}]$, $[C_d] = [c_{d(kl)}]$, and $[K_d] = [k_{d(kl)}]$, where $(k, l = 1, \ldots, 11)$, respectively. These matrices are functions of ω, the excitation frequency. The input force excitation vectors for $Q_l(i\omega)$ are defined as follows: for input front tires and input rear tires, we have $Q_{10}(i\omega) = (i\omega c_{10} + k_{10})q_0(i\omega)$ and $Q_{11}(i\omega) = (i\omega c_{11} + k_{11})q_0(i\omega)$, respectively. By substituting these values into Equation (30), we can obtain the displacement values for each degree of freedom (DOF) of the body segments and wheelchair components. Next, let us examine Equation (31). The term $[-\omega^2[M_d] + i\omega[C_d]+[K_d]]$ in this equation represents the impedance matrix that evaluates the mechanical responses of the human and vehicle frames. This impedance matrix can be expressed as transfer function matrices, as shown below. $\{q(i\omega)\}$ and $\{Q(i\omega)\}$ are the corresponding complex Fourier transform vectors of $q_k(i\omega)$ and $Q_l(i\omega)$, respectively, and ω represents the excitation frequency. By substituting these values into Equation (32), we obtain

$$\frac{q_k(i\omega)}{Q_l(i\omega)} = \frac{1}{-\omega^2 m_{d(kl)} + i\omega c_{d(kl)} + k_{d(kl)}} = D_{kl}(i\omega) \quad (k, l = 1, \ldots, 11), \tag{32}$$

where $D_{kl}(i\omega)$ represents the response at the mass k per unit force excitation at l. The matrix D_{kl} is derived from the equations of the mass, damping, and stiffness matrices. Its

inverse, as shown in Equation (33), becomes the transfer function $\{y_k(i\omega)\}$. This yields a set of matrix equations:

$$\begin{Bmatrix} q_1(i\omega) \\ q_2(i\omega) \\ q_3(i\omega) \\ \vdots \\ q_{11}(i\omega) \end{Bmatrix} = \begin{Bmatrix} D_{11} & D_{12} & \dots & D_{1(11)} \\ D_{21} & D_{22} & \dots & D_{2(11)} \\ D_{31} & D_{32} & \dots & D_{3(11)} \\ \vdots & \vdots & \ddots & \vdots \\ D_{(11)1} & D_{(11)2} & \dots & D_{(11)(11)} \end{Bmatrix} \begin{bmatrix} u_{11} & u_{12} & \dots & u_{1(11)} \\ u_{21} & u_{22} & \dots & u_{2(11)} \\ u_{31} & u_{32} & \dots & u_{3(11)} \\ \vdots & \vdots & \ddots & \vdots \\ u_{(11)1} & u_{(11)2} & \dots & u_{(11)(11)} \end{bmatrix}^T \begin{Bmatrix} F_1 \\ F_2 \\ F_3 \\ \vdots \\ F_{11} \end{Bmatrix}, \quad (33)$$

$$\begin{Bmatrix} y_1(i\omega) \\ y_2(i\omega) \\ y_3(i\omega) \\ \vdots \\ y_{11}(i\omega) \end{Bmatrix} = \begin{bmatrix} u_{11} & u_{12} & u_{13} & \dots & u_{1(11)} \\ u_{21} & u_{22} & u_{23} & \dots & u_{2(11)} \\ u_{31} & u_{32} & u_{33} & \dots & u_{3(11)} \\ \vdots & \vdots & \vdots & \ddots & \vdots \\ u_{(11)1} & u_{(11)2} & u_{(11)3} & \dots & u_{(11)(11)} \end{bmatrix} \begin{Bmatrix} q_1(i\omega) \\ q_2(i\omega) \\ q_3(i\omega) \\ \vdots \\ q_{11}(i\omega) \end{Bmatrix}. \quad (34)$$

As outlined above, $[u_{kl}(i\omega)]$ $(k, l = 1, \dots, 11)$ is an 11-by-11 matrix representing the shape mode with 121 possible contributions. By using $\{y_k(i\omega)\}$ and setting the input force vectors $\{q_k(i\omega)\}$, we can determine the displacement values for each degree of freedom (DOF) of the body segments and wheelchair components from Equation (34).

3.7. **Approaches for solving the equations of motion in MDOF.** This section discusses the various approaches used to solve the equations of motion (EOMs) in the multiple degrees of freedom (MDOF) system. In this study, the frequency-domain (FD) method is employed, focusing on the system's steady-state response. The model's responses are compared with published results of experimental measurements of whole-body vibration, which serve as the benchmark. The proximity of the model results to the benchmark is quantified using goodness-of-fit, a statistical technique that evaluates the prediction accuracy of each model configuration.

3.7.1. *Transmissibility.* Transmissibility, also known as displacement ratio, is defined as the ratio of the displacement at a point on the body to the displacement at the seat. In this study, three key attributes of the responses are evaluated for transmissibility. For instance, the transmissibility can be represented as

$$\textit{Transmissibility} = \frac{|y_k(i\omega)|}{|y_0(i\omega)|}, \quad k = 1, \dots, 11, \quad (35)$$

where $|y_k(i\omega)|$ represents the magnitudes of displacement response from the occupant's body part and wheelchair part (m_i), and $|y_0(i\omega)|$ represents the magnitudes of input excitation on the wheelchair.

3.7.2. *Goodness-of-fit (ϵ).* Goodness-of-fit (ϵ) is a statistical technique used to measure and evaluate the prediction accuracy of each model setup by comparing simulation results against published experimental values. Equation (36), shown below [16], is employed to calculate the ratio of the root-mean-square error of the test results to the mean value of the published data, representing the goodness-of-fit:

$$\epsilon = 1 - \frac{\sqrt{\frac{\sum_{m=1}^{N}(\tau_m - \tau_c)^2}{N-2}}}{\frac{\sum_{m=1}^{N}\tau_m}{N}}. \quad (36)$$

In Equation (36), τ_m represents the test datum, τ_c denotes the calculated result obtained from each model, and N corresponds to the number of test data points utilized in the

comparison. The quantity ϵ is defined as the ratio of the root-mean-square error of the test results to the mean value of the published data. It serves as a statistical measure to evaluate the accuracy of the prediction obtained from each model. As ϵ approaches 1, it indicates a higher degree of conformity between the predicted results and the published data, thus yielding a more reliable fit.

4. **Results and Discussion.**

4.1. **Validation of the 11-DOF model with different types of cushions.** The displacement ratio responses from the thorax to the pelvis versus input frequency obtained from our 11-DOF model with different types of cushions, according to the input parameters listed in Tables 1 and 2, are shown in Figure 2. The first peak value occurs at approximately 3 [Hz]. Superimposed on the figure is the experimental curve derived by Patil and Palanichamy [24]. The test results indicate that our model is of high quality, as it exhibits good agreement with the corresponding models in the literature. The input parameters presented in Tables 1 and 2 have a significant impact on the effectiveness of the results obtained in the study. These parameters define the characteristics of the mechanical system and the human occupant, influencing the dynamic response and transmissibility of vibrations. In Table 1, the parameter values of the occupant model are listed. These values determine the masses, damping constants, and spring constants of the individual components representing the occupant's body. By specifying these parameters, the model captures the resilient characteristics of the connective tissues between the body segments. The accuracy and appropriateness of these parameter values directly affect the realism and reliability of the occupant model's response to vibrations. Similarly, Table 2 provides the parameter values for the manual wheelchair. These values define the masses, damping constants, and spring constants of the various components of the wheelchair system, including the seat, chair frame, and tires. The selection of these parameter values reflects the physical properties and behavior of the wheelchair under vibrational excitation. The accuracy and appropriateness of these values influence the dynamic characteristics of the wheelchair-occupant system and its response to vibrations. It should be noted that the input magnitude of vibration, denoted as $y_0 = 5.0$ [mm], is also an important parameter specified in Table 2. This parameter represents the amplitude of the input wave, indicating the magnitude of the applied vibrations. The chosen

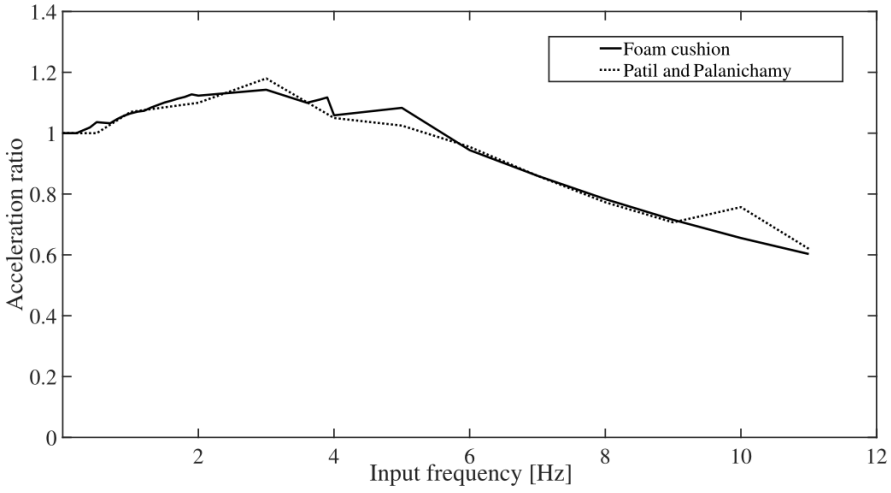

FIGURE 2. Thorax-to-pelvis displacement ratios on foam-based wheelchair cushions

value directly affects the intensity of the vibrations experienced by the occupant and, consequently, the resulting dynamic response. By accurately defining and selecting these input parameters, the study ensures a realistic representation of the wheelchair-occupant system and its response to vertical vibrations. Any variations or inaccuracies in these parameters could lead to different outcomes and impact the effectiveness of the results. In the simulation results section, it is recommended to include more comprehensive results, particularly in terms of comparisons. By including additional comparative analyses, such as comparing different seat parameters or variations in input vibration characteristics, a more thorough evaluation and understanding of the findings can be achieved. These comparative results would provide valuable insights into the effects of different factors on the transmissibility and dynamic responses of the wheelchair-occupant system, enhancing the overall significance and applicability of the study.

4.2. **Comparison of predictions and measurements for foam-based cushion transmissibility with goodness-of-fit.** This section presents a comparison between the transmissibility results obtained from the model and those from laboratory experiments [8], using a statistical technique known as goodness-of-fit [16]. Figure 3 shows the comparison of maximum transmissibility and corresponding frequency values between the measured values from the actual roadcourse test and the predicted values of the 11-DOF model for foam-based seating systems, calculated using Equations (1)-(36). The model-derived responses of the seat cushion to vibrations closely match the measured values obtained from experimental testing of a foam-based cushion by Garcia-Mendez [8], with a goodness-of-fit of 84[%] [14]. The comparison reveals that the predicted and measured values of the foam-based cushion exhibit similar amplitude ratios of maximum transmissibility at 1.14 for 2 [Hz] and 1.18 for 3.16 [Hz] [8] (with the occupant seated on a foam-based cushion). This indicates that the foam-based cushion helps reduce amplified vibrations within the frequency range harmful to humans, as observed from both the measured and predicted responses. The 11-DOF model predicts lower estimated seat transmissibility during wheelchair propulsion in the frequency range of 3 to 15 [Hz], which aligns well with the underestimated measured seat transmissibility during the roadcourse test. The

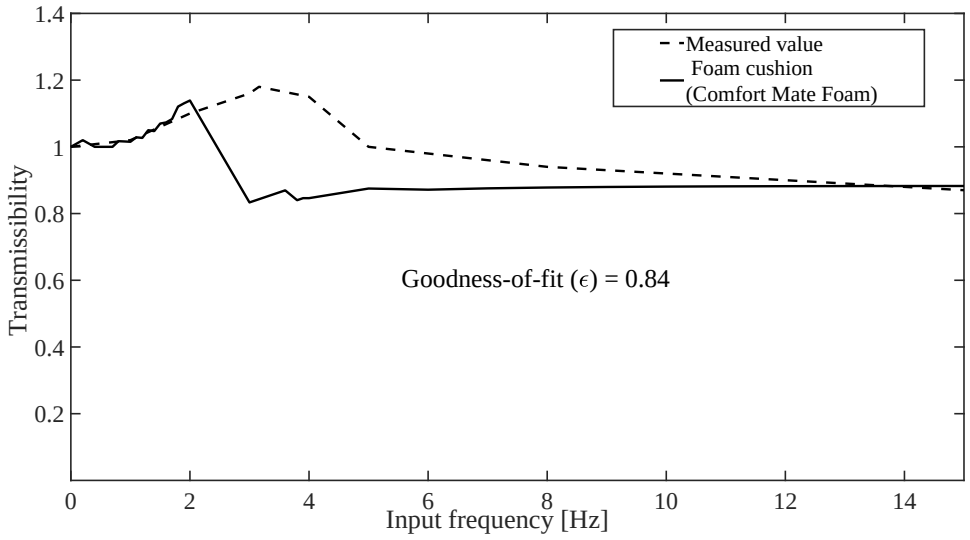

FIGURE 3. Comparison between measured and predicted values of seat transmissibility for foam cushion

comparison between measured and predicted seat transmissibility values for the foam-based cushion provides valuable insights. However, there are certain limitations in the study that should be addressed, along with potential future directions to enhance the model's understanding and applicability. One limitation is the focus solely on maximum transmissibility and corresponding frequency values. A more comprehensive analysis of the entire transmissibility response curve, covering the entire frequency range and examining variations in transmissibility at different frequencies, would provide a more thorough assessment of the model's performance. Quantitative analysis of the agreement between measured and predicted values would also be beneficial. In addition to the mentioned 84[%] goodness-of-fit, incorporating statistical measures such as mean absolute error or coefficient of determination (R-squared) would offer a more objective evaluation of the model's accuracy and reliability. Furthermore, relying solely on a single experimental dataset for validation has its limitations. Incorporating data from multiple independent studies would enhance the validation process and provide a better understanding of the model's performance across different setups and conditions.

In terms of future directions, validating the model with data from a wider range of foam-based cushion experiments would improve its generalizability. Considering variations in cushion design, material properties, and testing conditions would enhance the model's applicability for designing and evaluating foam-based seating systems. Additionally, investigating the transmissibility behavior of other types of seating systems and cushions would be valuable. Comparing model predictions with experimental data for different cushions would provide insights into their performance and aid in selecting appropriate cushions for specific applications. Moreover, exploring the effect of different input vibrations on transmissibility, such as random vibrations or vibrations during specific activities, would provide a more realistic assessment.

4.3. **Biodynamic evaluation of the wheelchair and occupant model.** In the biodynamic evaluation of the wheelchair and occupant model, researchers have extensively studied the biodynamic responses of seated individuals to vertical vibrations, focusing on the transmissibility of magnitudes and phases. Various mathematical models of different complexities have been developed, and extensive data has been collected to characterize these response functions under different experimental conditions. This paper specifically includes data compiled using mathematical models based on well-defined assumptions. Figures 4-7 illustrate the steady-state responses of the wheelchair seat and various body parts to vertical vibrations in the frequency range of 0.5 to 15 [Hz]. These figures depict the amplitude and phase ratios of the response amplitude to the input amplitude. Specifically, Figure 4 presents a comparison of the vibration transmissibility from the excitation to the wheelchair occupant's head and torso for tests conducted on a foam cushion. The solid line represents the transmissibility to the head, while the dotted line represents the transmissibility to the torso.

Similarly, Figure 5 examines the vibration transmissibility from the excitation source to the wheelchair occupant's back and seat. Here, the solid line represents the transmissibility to the back, while the dotted line represents the transmissibility to the seat. Moving on to Figure 6, it displays the comparison of vibration transmissibility from the excitation to the wheelchair occupant's thorax and diaphragm during the tests on the foam cushion. The solid line corresponds to the transmissibility to the thorax, while the dotted line represents the transmissibility to the diaphragm. Finally, Figure 7 focuses on the comparison of vibration transmissibility from the excitation to the wheelchair occupant's abdomen and pelvis. The solid line indicates the transmissibility to the abdomen, while the dotted line depicts the transmissibility to the pelvis.

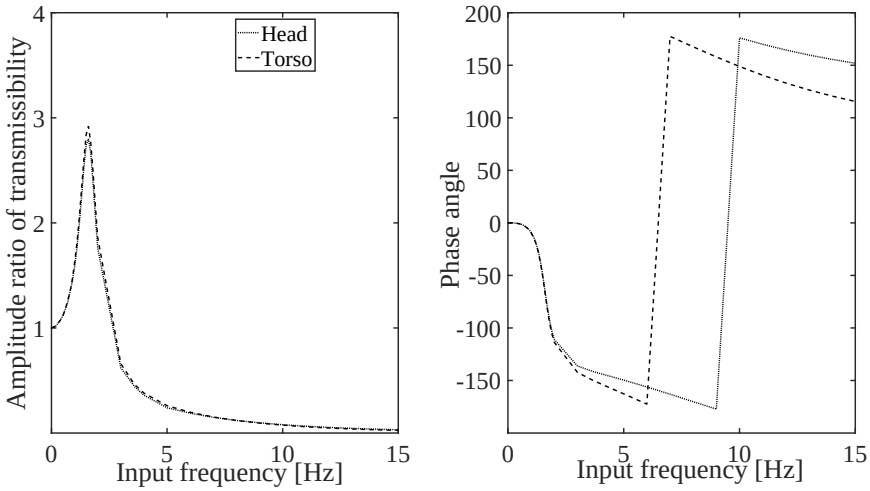

FIGURE 4. Comparison of vibration transmissibility from excitation to wheelchair occupant's head and torso for tests on foam cushion

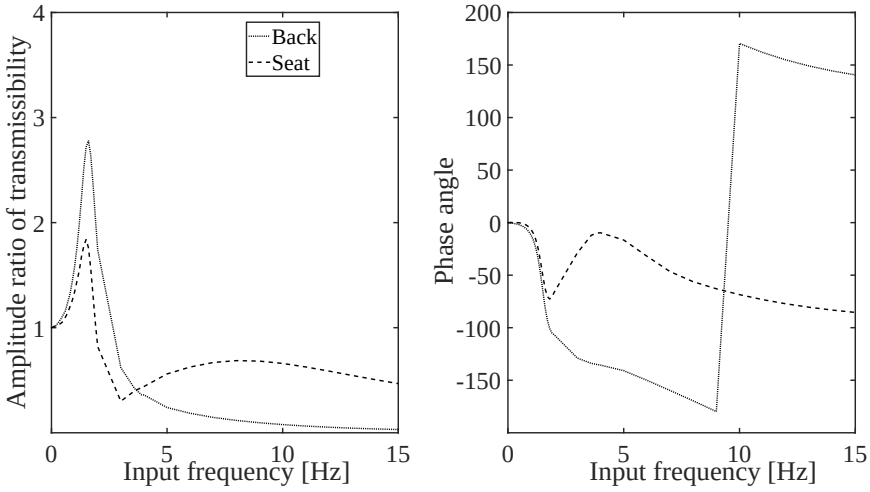

FIGURE 5. Comparison of vibration transmissibility from excitation to wheelchair occupant's back and seat for tests on foam cushion

The peak responses of the head, back, torso, thorax, diaphragm, abdomen, and pelvis occur at 1.6 [Hz], with amplitude ratios of transmissibility equal to 2.8, 2.78, 2.92, 2.9, 2.84, 2.78, and 2.62, respectively. The torso experiences the highest response among all body segments, with an amplitude ratio of transmissibility equal to 2.92. At higher frequencies (0.5 to 15 [Hz]), the average response of all body parts is approximately 0.0094. Comparing the amplitude ratios of transmissibility, it is observed that they occur at 1.6 [Hz], which is about 7% higher than the amplitude ratio at which the seat response occurs (1.5 [Hz]). This highlights the importance of modeling the body parts, including the wheelchair seat, and the need to design suspension systems based on the amplitude ratios of the body parts to ensure human comfort.

Analyzing the frequency response curves in Figures 4-7, it can be seen that at low frequencies below 1 [Hz], which are far from the natural frequency, the transmissibility is approximately 1. This implies that the amplitude of displacement is equal to the excitation displacement. Therefore, if the wheelchair is subjected to high levels of vibration, the transmitted force to the occupant will also be equally high, without any reduction. As

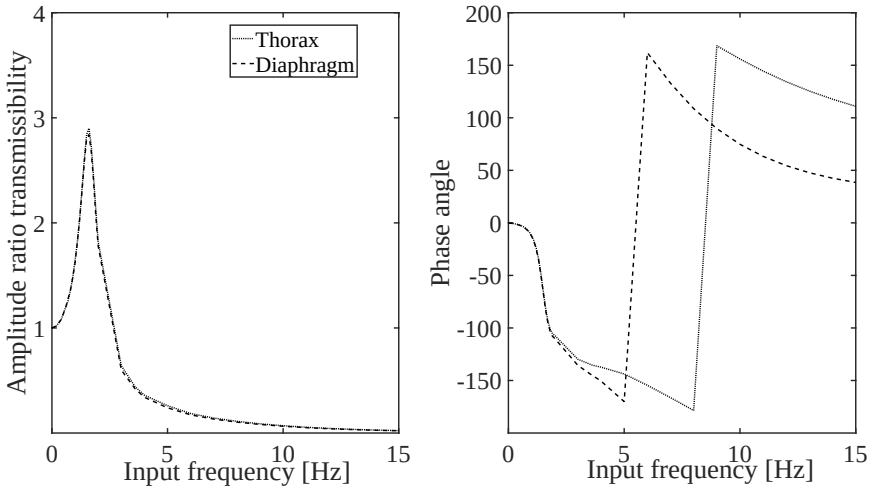

FIGURE 6. Comparison of vibration transmissibility from excitation to wheelchair occupant's thorax and diaphragm for tests on foam cushion

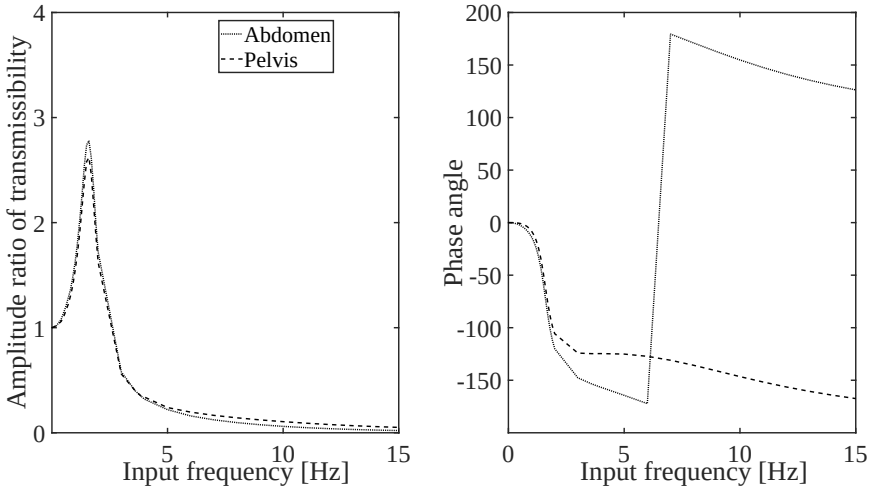

FIGURE 7. Comparison of vibration transmissibility from excitation to wheelchair occupant's abdomen and pelvis for tests on foam cushion

the excitation frequency approaches the natural frequency (1 to 1.6 [Hz]), the transmissibility value increases and approaches its peak value. In cases where the transmissibility exceeds 1, the transmitted force becomes greater than the excitation force, resulting in the transmitted force to the occupant being 2.6 to 2.9 times the excitation force, which is a dangerous situation and should be avoided in engineering. Transmissibility is defined as the ratio of the transmitted force to the excitation force. At frequencies below 1.6 [Hz], as the excitation frequency increases, the transmissibility decreases, indicating that the transmitted force is lower than the excitation force. This implies that the transmitted force decreases as the excitation frequency increases beyond 1.6 [Hz]. Furthermore, the frequency response curves demonstrate that at low frequencies, the transmissibility is approximately 1, indicating a direct relationship between the excitation and transmitted forces. Near the natural frequency, the transmissibility increases and can exceed 1, resulting in amplified transmitted forces. At frequencies higher than 1.6 [Hz], the transmissibility decreases, leading to reduced transmitted forces compared to the excitation forces.

While this study provides valuable insights into the vibration transmissibility of different body parts, there are limitations and future directions to consider for further improvement. One limitation is the focus on a specific frequency range (0.5 to 15 [Hz]) for evaluating vibration transmissibility. Although this range covers a significant portion of vibrations experienced during wheelchair use, it would be beneficial to investigate transmissibility behavior at higher frequencies as well. High-frequency vibrations may have different effects on the body and can impact occupant comfort and safety. Expanding the frequency range of the study would provide a more comprehensive understanding of transmissibility characteristics across a wider spectrum of vibrations. Additionally, it is important to consider the variability in body types and anthropometric dimensions among wheelchair users. The current study does not account for individual differences in body characteristics, which can influence transmissibility responses. Future research should incorporate a more diverse range of anthropometric data to capture the effects of individual variations on vibration transmissibility. This would improve the accuracy and applicability of the model for a broader population of wheelchair users. Furthermore, exploring the effects of different seating configurations and cushion types on vibration transmissibility would be beneficial. Variations in seat design, cushion materials, and suspension systems can significantly impact the transmission of vibrations to the occupant. Evaluating and comparing different seating configurations and cushion types would provide insights into their relative performance and assist in designing more effective and comfortable wheelchair systems [8, 25, 26]. Moreover, while the study primarily focuses on the steady-state responses of different body parts, investigating transient responses would be valuable as well. Transient vibrations, such as those encountered during wheelchair propulsion or when encountering obstacles, can have different effects on the body compared to steady-state vibrations. Incorporating transient vibration analyses would provide a more comprehensive understanding of the dynamic behavior of the wheelchair-occupant system and help identify potential issues or discomfort during specific activities [8]. Additionally, experimental validation of the model predictions would be beneficial. Comparing the predicted transmissibility values with experimental measurements obtained from actual wheelchair users would provide direct validation and enhance confidence in the model's accuracy. This would involve conducting controlled experiments with human participants and measuring the vibration responses of different body parts with the human subject seated in a wheelchair under various conditions. Lastly, while the study focuses on amplitude ratios of transmissibility, analyzing the phase relationships between input vibrations and the responses of different body parts would also be worthwhile. Investigating phase shifts and phase differences can reveal important dynamics and synchronization effects between vibrations and the body's response, which can influence the perception of vibration and overall occupant comfort.

5. **Conclusion.** In this study, we have presented a linear differential equation model with 11 degrees of freedom, which effectively predicts how foam-based cushions behave in terms of vibration and shock absorption. The model was solved using the modal analysis method and its performance was evaluated by comparing its predictions with well-established experimental data from the industry literature. Our findings demonstrate that the torso has the highest amplitude ratios of transmissibility compared to other body parts. The modeling approach introduced in this research has great potential for advancing wheelchair design and analyzing vibrating systems. Future research can build upon this model by incorporating more complex geometries and material properties, while also conducting experimental validation to confirm its predictive capabilities. Although the biodynamic evaluation of the wheelchair and occupant model has provided valuable insights, there

are still opportunities for further improvement. By addressing the limitations discussed in this study and pursuing the suggested future directions, we can enhance the accuracy, reliability, and applicability of the model. Ultimately, these advancements will lead to a deeper understanding of vibration transmissibility and contribute to the development of wheelchair systems that prioritize occupant comfort and safety.

Acknowledgment. This material is the result of work supported by JSPS KAKENHI Grant Number JP21K03930.

REFERENCES

[1] M. L. Toro-Hernández, L. Alvarez, M. C. Vargas-Chaparro and M. Goldberg, Final year students' knowledge on basic manual wheelchair provision: The state of occupational therapy programs in Colombia, *Occupational Therapy International*, vol.2020, pp.1-8, Article ID 3025456, 2020.

[2] A. M. Geers, E. C. Prinsen, D. J. van der Pijl, A. Bergsma, J. S. Rietman and B. F. J. M. Koopman, Head support in wheelchairs (scoping review): State-of-the-art and beyond, *Disability and Rehabilitation: Assistive Technology*, DOI: 10.1080/17483107.2021.1892840, 2021.

[3] E. Wolf, J. Pearlman, M. L. Boninger and R. A. Cooper, Health risks of vibration exposure to wheelchair users in the community, *The Journal of Spinal Cord Medicine*, vol.31, no.4, pp.361-369, 2008.

[4] O. Lariviere, D. Chadefaux, C. Sauret and P. Thoreux, Vibration transmission during manual wheelchair propulsion: A systematic review, *Vibration*, vol.4, no.2, pp.444-481, 2021.

[5] Y. Garcia-Mendez, J. L. Pearlman, M. L. Boninger and R. A. Cooper, Health risks of vibration exposure to wheelchair users in the community, *The Journal of Spinal Cord Medicine*, vol.36, pp.365-375, 2013.

[6] M. J. Griffin, Discomfort from feeling vehicle vibration, *Vehicle System Dynamics*, vol.45, nos.7-8, pp.679-688, 2007.

[7] Y. Garcia-Mendez, J. Pearlman, M. L. Boninger and R. A. Cooper, Whole-body vibration exposure in manual wheelchair users: Influence of wheelchair components, *Medical Engineering and Physics*, vol.52, pp.1-7, 2018.

[8] Y. Garcia-Mendez, J. L. Pearlman, R. A. Cooper and M. L. Boninger, Dynamic stiffness and transmissibility of commercially available wheelchair cushions using a laboratory test method, *Journal of Rehabilitation Research & Development*, vol.49, no.1, pp.7-22, 2012.

[9] T. Waga, S. Ura, M. Nagamori, H. Uchiyama and A. Shionoya, Influence of material on wheelchair vibrations, *The 13th Conference of the International Sports Engineering Association*, pp.1-6, 2020.

[10] F. Chénier and R. Aissaoui, Effect of wheelchair frame material on users' mechanical work and transmitted vibration, *BioMed Research International*, vol.2014, pp.1-12, Article ID 609369, 2014.

[11] P. Weerapong, K. Hashikura, M. A. S. Kamal and K. Yamada, A model for the response of an occupant and wheelchair system subjected to vertical vibrations, *International Journal of Innovative Computing, Information and Control*, vol.17, no.6, pp.1823-1841, 2021.

[12] P. Weerapong, K. Hashikura, M. A. S. Kamal and K. Yamada, A biodynamic model of wheelchair with changeable seat cushions subjected to vertical vibrations, *ICIC Express Letters*, vol.16, no.1, pp.33-41, 2022.

[13] P. Weerapong, K. Hashikura, M. A. S. Kamal, I. Murakam and K. Yamada, Analysis of model output in the simulation of a wheelchair-occupant system subjected to vibration, *ICIC Express Letters, Part B: Applications*, vol.14, no.4, pp.389-398, 2023.

[14] P. Weerapong, K. Hashikura, M. A. S. Kamal, I. Murakam and K. Yamada, Simulated response analysis: Modelling a wheelchair occupant system subjected to vibration, *International Journal of Innovative Computing, Information and Control*, vol.19, no.2, pp.307-323, 2023.

[15] A. Asgharnia, H. Schwartz and M. Atia, Learning multi-objective deception in a two-player differential game using reinforcement learning and multi-objective genetic algorithm, *International Journal of Innovative Computing, Information and Control*, vol.18, no.6, pp.1667-1688, 2022.

[16] C. C. Liang and C. F. Chiang, A study on biodynamic models of seated human subjects exposed to vertical vibration, *International Journal of Industrial Ergonomics*, vol.36, pp.869-890, 2006.

[17] N. F. Nangolo, J. Soukup, L. Rychlíková and J. Skocăilas, A combined numerical and modal analysis on vertical vibration response of railway vehicle, *Procedia Engineering*, vol.96, pp.310-319, 2014.

[18] J. Schwochow and G. Jelcic, Automatic operational modal analysis for aeroelastic applications, *Proc. of the 6th International Operational Modal Analysis Conference (IOMAC)*, pp.1-14, 2015.
[19] O. Lariviere, D. Chadefaux, C. Sauret and P. Thoreux, Experimental modal analysis of a standard wheelchair: A preliminary study, *Computer Methods in Biomechanics and Biomedical Engineering*, vol.23, DOI: 10.1080/10255842.2020.1813416, 2020.
[20] O. Lariviere, D. Chadefaux, C. Sauret, L. Kordulas and P. Thoreux, Modal characterization of manual wheelchairs, *Vibration*, vol.5, no.3, pp.442-463, 2022.
[21] M. F. Hikmawan and A. S. Nugraha, Analysis of electric wheelchair passenger comfort with a half car model approach, *ICSEEA 2016 International Conference on Sustainable Energy Engineering and Application*, pp.76-80, 2016.
[22] M. R. Hatch, *Vibration Simulation Using MATLAB and ANSYS*, Chapman and Hall/CRC, New York, 2001.
[23] G. Strang, *Introduction to Linear Algebra*, 2nd Edition, Wellesley-Cambridge Press, Wellesley, 1998.
[24] M. K. Patil and M. S. Palanichamy, A mathematical model of tractor-occupant system with a new seat suspension for minimization of vibration response, *Applied Mathematical Modelling*, vol.12, pp.63-71, 1988.
[25] J. Marcondes, K. Hatton, J. Graham and H. Schueneman, Effect of temperature on the cushioning properties of some foamed plastic materials, *Packaging Technology and Science*, vol.16, no.5, pp.231-237, 2003.
[26] M. Tomina, M. A. Lengyel, R. D. Párizs and A. Kmetty, Measuring and mathematical modeling of cushion curves for polymeric foams, *Polymer Testing*, vol.117, 107837, 2023.

Author Biography

Pongtep Weerapong received his B.E. degree in Materials Engineering in 2005 and his M.E. degree in Polymer Processing Engineering in 2007, both from King Mongkut's University of Technology Thonburi (KMUTT), Thailand. He completed his Ph.D. in Mechanical Science and Technology at Gunma University, Japan, in 2023. He is currently an associate professor at Nakhon Si Thammarat Rajabhat University. His current research interests include assistive technology for children with disabilities and whole-body vibration.

Mitsuki Katahira received the B.E. degree in Mechanical Science and Technology from Gunma University, Japan in 2022. He is now a master course student at Gunma University, Japan. His research interests include assistive technology for children with disabilities and whole-body vibration.

Kotaro Hashikura received the B.S. degree in Mechanical Engineering from Kyushu Institute of Technology, Fukuoka, Japan, 2006; the M.S. degree of Informatics from Kyoto University, Kyoto, Japan, 2010; and the Doctor degree in Engineering from Tokyo Metropolitan University, Tokyo, Japan, 2014. From 2014 until 2018, he had been a Project Research Associate at the Faculty of System Design, Tokyo Metropolitan University. Dr. Hashikura is currently a full-time professor at Division of Mechanical Science and Technology, Gunma University, Japan. His research interests include time-delay-related control techniques, such as deadbeat, preview-prediction and repetitive controls. He is a member of IEEE, ISCIE and SICE.

Md Abdus Samad Kamal received the B.Sc. degree in Electrical and Electronic Engineering from Khulna University of Engineering and Technology (KUET), Khulna, Bangladesh in 1997; Master and Doctor degrees from Graduate School of Information Science and Electrical Engineering from Kyushu University, Japan in 2003 and 2006, respectively. He was a post-doctoral fellow in Kyushu University till November 2006. Dr. Kamal is currently a full-time professor at Division of Mechanical Science and Technology, Gunma University, Japan. His current research interests are reinforcement learning, intelligent transportation systems, and multiagent systems. He is a member of IEEE and SICE.

Iwanori Murakami received his Ph.D. Eng. from Gunma University in 1997. He is currently an associate professor at Gunma University. His research interests include robotics, applied electromagnetics and machines, and superconducting levitation applications.

Kou Yamada received B.S. and M.S. degrees from Yamagata University, Yamagata, Japan in 1987 and 1989, respectively, and a Dr. Eng. degree from Osaka University, Osaka, Japan in 1997. From 1991 to 2000, he was with the Department of Electrical and Information Engineering, Yamagata University, Yamagata, Japan as a research associate. From 2000 to 2008, he was an associate professor in the Department of Mechanical System Engineering, Gunma University, Gunma, Japan. Since 2008, he has been a professor in the Division of Mechanical Science and Technology, Gunma University, Gunma, Japan. His research interests include robust control, repetitive control, process control, and control theory for inverse systems and infinite-dimensional systems. Dr. Yamada received the 2005 Yokoyama Award in Science and Technology, the 2005 Electrical Engineering/Electronics, Computer, Telecommunication, and Information Technology International Conference (ECTI-CON2005) Best Paper Award, the Japanese Ergonomics Society Encouragement Award for an Academic Paper in 2007, the 2008 Electrical Engineering/Electronics, Computer, Telecommunication, Information Technology International Conference (ECTI-CON2008) Best Paper Award, and the 4th International Conference on Innovative Computing, Information and Control Best Paper Award in 2009, the 14th International Conference on Innovative Computing, Information and Control Best Paper Award in 2019, and Outstanding Achievement Award from Kanto Branch of Japanese Society for Engineering Education in 2022 and JSME (The Japan Society of Mechanical Engineers) Education Award in 2023. He is a member of IEEE and SICE, and a fellow of JSME.